STUDY ON HEAT TRANSFER OF WAXY CRUDE OIL MELTING PHASE CHANGE BASED ON A NOVEL MODEL

by

Ying XU[a], Kaijing ZHANG[a], Lijun LIU[c], Pengli GE[b], Xiaoyan LIU[a], Zhiguo WANG[a], and Haiqian ZHAO[a]*

[a]Northeast Petroleum University, Daqing city, China
[b]Research Institute of Petroleum Engineering, SINOPEC Northwest Oilfield Company, Urumqi, Xin Jiang, China
[c]Changshu Institute of Technology, Changshu city, China

The study of phase change heat transfer of crude oil melting is important for pre-heating and restarting of pipelines. Combining the characteristics of waxy crude oil characteristics of waxy crude oil melting, a novel mathematical model was established, which can accurately describe the non-linear release of latent heat, liquid-solid interface changes, natural convection, and other key heat transfer problems. In the process of heating and melting, the variation law of the solid-phase interface position in the pipe at different initial solidification states was analyzed. The results showed that in the partially solidified pipeline, the liquid crude oil in the pipeline has a higher temperature at the initial heating stage, and continuously loses heat to the low temperature crude oil, resulting in a decline in the liquid-phase ratio at the initial stage. Because crude oil was affected by different degrees of radial thermal resistance, latent heat release and porous medium characteristics at different positions of the pipeline, the temperature drop curves of the crude oil varies greatly.

Key words: *waxy crude oil, melting law, melting time, liquid rate,*
condensate oil interface

Introduction

Waxy crude oils often use heating and warming to maintain their fluidity during storage and transportation due to their high freezing point, high paraffin point and high viscosity. During pipeline transportation, waxes in crude oil precipitate first as heat loss increases, and as the wax crystals increase in size, it is gradually deposited in the lower part of the pipeline, reducing the flow area. Therefore, furnace heating and electric heating at the wellhead are often used. The phase change heat transfer phenomenon of crude oil melting often occurs simultaneously with the heating procedures used in waxy crude oil gathering and transportation systems. For example, if intermediate stations and transfer lines in long distance pipelines are heated to raise the temperature, the gelled crude oil will continue to melt. The condensate must also be heated before returning to the storage tank, and the experiment can be repeated after the cooling

_____

and solidification process is complete. Therefore, understanding the melt phase change mechanism of waxy crude oils is essential to guide crude oil transportation and extraction.

As shown in fig. 1, the melt heat exchange process of crude oil is extremely complex due to the presence of wax, involving a variety of physical phenomena such as latent heat absorption, phase interface movement, liquid-solid/solid-liquid phase change, heat transfer mode conversion and fluid-solid coupling [1-5]. With a mobile phase interface, the phase change melting of crude oil is a Stefan problem, and the main issues that need to be resolved during the modeling process are latent heat absorption, interface position change, the influence of natural convection and heat transfer, and the description of non-Newtonian properties of crude oil [6-9].
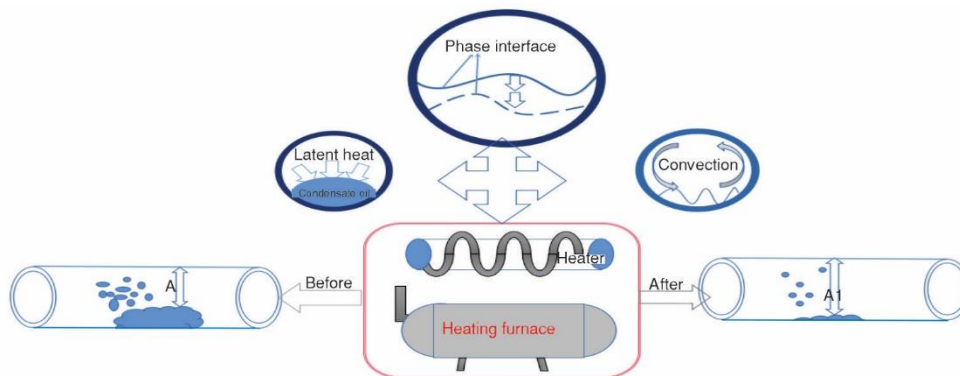

Figure 1. Heating and melting of crude oil

To cope with the latent heat of phase shift in crude oil, a DSC curve was utilized. Drissi *et al.* [10] used the DSC method to determine the latent heat of phase transition material and investigated the impact of various masses and heating rates. Through a DSC experiment, Sun *et al.* [11] was able to determine the latent heat and phase transition temperature of the melting process of phase change materials. Kousksou *et al.* [12] investigated the DSC melting of eutecticsalts.

Phase change heat transfer problems is characterised by the existence of a time-varying phase change interface in the solution domain. For pure substances, the moving interface is apparent at a certain phase change temperature. For impure substances, melting/solidification occurs over a range of temperatures. Therefore, the phase change moving interface is a two-phase region of solid-liquid coexistence, latent heat release or absorption. Chen and Jiang [13] developed a similar 1-D melting model for RT60 paraffin under Type I boundary conditions, without considering the effect of convective heat transfer in the molten fraction. Numerical simulations were carried out using fluent software. The variation of temperature and fluid rate with time was obtained. The fluid parameters were set to a paraffin melting temperature of 58~60 °C and a latent heat of melting of 214 kJ/kg. Jin *et al.* [14] developed a mathematical model considering only axial heat transfer, with an inner tube filled with stearic acid and an outer tube filled with stearic acid as a heat transfer fluid flowing along the longitudinal direction. The smooth simulation results showed the temperature field in the calculated region at different moments during solidification.

The change in viscosity with temperature [15-18] was typically used to describe how non-Newtonian properties of crude oil affected the phase transition process. Ma *et al.* [15] created a novel electro treatment system and evaluated the rheological characteristics of waxy crude oil. Electrical treatment increased the waxy crude oil's ability to flow in the cold. A

method for determining the viscosity of crude oil was developed based on the concepts of non-Newtonian fluid mechanics and rheology. Nine samples of crude oil were examined by Lize *et al*. [16] to determine their densities, water contents, wax contents (1-D chromatography), pour points, yield stresses, and wax-like appearance temperatures. The findings demonstrated that increasing the pour point of crude oil was made possible by the low concentration of *n*-alkanes in aromatic compounds.

Based on the phase change properties of wax-containing crude oil melting wax crystal, a new phase change heat transfer model was developed in this research. The pipeline's crude oil was separated into zones for the liquid phase, solid phase, and liquid-solid mixing. The numerical solution was implemented using the finite volume method. The study's findings provided a theoretical framework on which to build an oil transfer strategy for a long-distance pipeline.

Physical model of wide phase transition zone

Analysis of phase behavior change in melting process

The use of a polarizing microscope was used to conduct the oil melting phase experiment. The sample's wax precipitation point was 44 °C, and the oil condensation point was 32 °C. In the experiment, in order to ensure the uniform thickness of oil film and reduce the influence of oil film thickness on wax crystal microscopy data, a special slide with a central groove of 6 mm in diameter and 0.15 mm in depth was prepared, and the volume of oil sample added in each drop was precisely controlled to ensure the uniform thickness of oil film spread after each drop of oil sample. To determine the phase distribution of the sample at a typical temperature, such as in fig. 2, the condensate oil sample was placed on the thermostatic heating platform of the microscope, and a temperature rise and melting experiment was conducted.
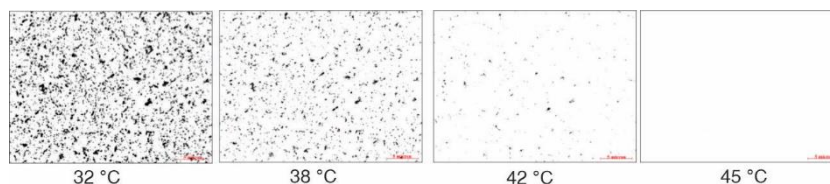

Figure 2. The phase state of wax crystals changes at typical temperatures

As can be seen from fig. 2, when the temperature of the crude oil reached the freezing point, the entire crude oil sample lost its fluidity due to the formation of a strong cross-lattice structure between a large number of wax crystals. At this time, the small amount of liquid oil in the grid was basically at rest due to the restriction of the grid. When the crude oil was heated, the original wax crystal skeleton kept melting, the mesh effect gradually decreased, and the mobility of the melted crude oil and the crude oil in the pore space increased. At this point, the crude oil presented the characteristics of a porous medium. The aggregation point was the temperature of the crude oil corresponding to the disappearance of the grid properties of the porous medium during the heating process. Its determination was done by microscopic experimental pictures, using pixel tracking method, and several wax crystal points were randomly selected to observe the pixel position of each point during the heating process. When the grid structure disappeared, the wax crystal point position will change significantly due to the natural convection effect inside the crude oil during the heating process, so the temperature of the agglomeration point can be determined according to the displacement change of the wax crystal point. When the crude oil continues to be heated, the lattice structure disappeared and only a small

amount of wax crystals are suspended in the liquid crude oil, as shown in the wax crystal diagram at 42°C. When the temperature of the crude oil was higher than the wax evolution point, all the wax crystals melt away and all the crude oil samples were liquid.

Wide-phase interface partition model

According to the phase change of wax crystals, three changes in the heat transfer and flow patterns occur during melting:
– When the crude oil was below the freezing point, the whole lost its fluidity and the mode of heat transfer can be considered as pure heat conduction.
– When the temperature of the crude oil was between the freezing point and the coalescence point (the temperature at which porous structures was formed), which in this experiment was 38 °C, the crude oil showed the characteristics of a porous medium. A percolation model was used to describe its flow process.
– When the temperature of crude oil was higher than the wax point, all of the crude oil was liquid and the heat transfer was natural convection.

The 2-D physical heat transfer model of the overhead pipeline was shown in fig. 3 according to the different states of the crude oil and the transformation of the heat transfer mode of the crude oil. The center of the pipeline was the crude oil, the pipe and the insulating soil, from the inside out. The heat transfer of crude oil in the pipeline conforms to a wide phase transition zone, that was, the crude oil in the heated pipeline was divided into a solid phase zone, a liquid-solid mixed porous medium zone and a liquid phase zone from the inside to the outside. The heat transfer between the pipe and the insulation layer was heat conduction, and the heat transfer between the insulation layer and the ambient air was compound. The temperature of the constant temperature layer was chosen as 283.15 K. The following assumptions were made: the crude oil was considered as an incompressible

Figure 3. Physical model of overhead pipeline melting heating

fluid, the contact thermal resistance between the layers was ignored, and the thickness and thermal resistance of the heating tape were not considered, and the heat transfer was considered as unidirectional.
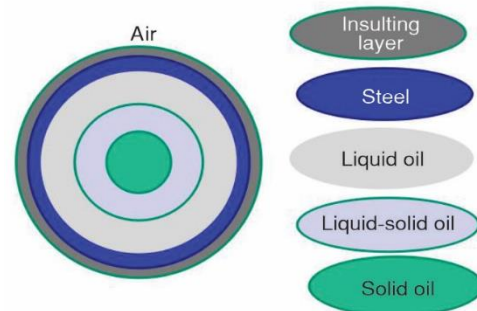
Mathematical model

Liquid phase zone

The liquid phase of crude oil in the pipeline contained the following three equations: continuity equation, momentum equation, and energy equation:

$$\frac{\partial \rho}{\partial t} + \frac{1}{r}\frac{\partial (\rho r u_r)}{\partial r} + \frac{1}{r}\frac{\partial (\rho u_\theta)}{\partial \theta} = 0 \tag{1}$$

$$\frac{\partial (\rho u_\theta)}{\partial t} + \frac{1}{r}\frac{\partial}{\partial \theta}(\rho u_\theta u_\theta) + \frac{1}{r}\frac{\partial}{\partial r}(\rho r u_r u_\theta) = \frac{1}{r}\frac{\partial}{\partial \theta}\left(\frac{\mu}{r}\frac{\partial u_\theta}{\partial \theta}\right) + \frac{1}{r}\frac{\partial}{\partial r}\left(\mu r \frac{\partial u_\theta}{\partial r}\right) + S_\theta \tag{2a}$$

$$\frac{\partial(\rho u_r)}{\partial t}+\frac{1}{r}\frac{\partial}{\partial\theta}(\rho u_\theta u_r)+\frac{1}{r}\frac{\partial}{\partial r}(\rho ru_ru_r)=\frac{1}{r}\frac{\partial}{\partial\theta}\left(\frac{\mu}{r}\frac{r}{\partial\theta}\right)+\frac{1}{r}\frac{\partial}{\partial r}\left(\mu r\frac{\partial u}{\partial r}\right)+S_r \qquad (2b)$$

$$S_\theta=-\frac{\partial p}{\theta}+\left(-\frac{\rho u_r u_\theta}{r}+\frac{2\mu}{r^2}\frac{\partial u_r}{\partial\theta}-\frac{u_\theta}{r^2}\right)+\text{g}\rho\beta(T-T_{\text{ref}})\sin\theta \qquad (2c)$$

$$S_r=-\frac{\partial p}{r}+\left(\frac{\rho u_\theta^2}{r}-\frac{2\mu}{r^2}\frac{\partial u_\theta}{\partial\theta}-\frac{\mu u_r}{r^2}\right)+\text{g}\rho\beta(T-T_{\text{ref}})\cos\theta \qquad (2d)$$

The specific heat capacity of crude oil at different temperatures was calculated using the DSC curve, and the heat source term was ignored in the energy control equation, and the equivalent specific heat capacity method was used to deal with the latent heat problem, where cp is transient equivalent specific heat capacity:

$$\frac{\partial(\rho T)}{\partial t}=\frac{\partial}{r^2\partial\theta}\left(\frac{\lambda_1}{c_p}\frac{\partial T}{\partial}\right)\frac{1}{r}\frac{\partial}{\partial r}\left(\frac{\lambda_1}{c_p}r\frac{\partial T}{\partial r}\right) \qquad (3)$$

When the oil temperature is higher than the wax precipitation point, $\lambda_t=\lambda_1$. When the temperature was between breaking point and the wax precipitation point, λt was determined by the following equation:

$$\varepsilon=1-\frac{T_{\text{x}}-T}{T_{\text{x}}-T_{\text{n}}} \qquad (3a)$$

$$\phi=1-\varepsilon \qquad (3b)$$

$$\lambda_t=\lambda_l\frac{2+\frac{s}{\lambda_l}+2\phi\left(\frac{\lambda_s}{\lambda_l}-1\right)}{2+\frac{\lambda_s}{\lambda_l}-\phi\left(\frac{\lambda_s}{\lambda_l}-1\right)} \qquad (3c)$$

Solid phase zone

The governing equation for the solid phase region was the energy equation, as shown in eq. (4), at which $\lambda_t=\lambda_s$.

$$\frac{\partial(\rho T)}{\partial t}=\frac{\partial}{r^2\partial\theta}\left(\frac{\partial T}{c_p\partial}\right)\frac{1}{r}\frac{\partial}{\partial r}\left(\frac{\lambda_s}{c_p}r\frac{\partial T}{\partial r}\right) \qquad (4)$$

Porous media zone

In this study, a wide phase transition partition model would be used in the porous media region. The equivalent thermal conductivity, λ_t, permeability, K, and shape coefficient, F_ε, were calculated by the liquid rate.

$$\frac{(r)}{\partial r}(u_r\cos\theta-u_\theta\sin\theta)+\frac{1}{\varepsilon}\sqrt{u^2+u^2}\left(\frac{\partial(\rho u_r)}{\partial r}+\frac{1}{r}\frac{\partial(\rho u_\theta)}{\partial\theta}+\frac{\rho u_r}{r}\right)=$$

$$=(-\varepsilon)\frac{\partial P}{\partial r}\cos\theta+\mu_e\left[\frac{\partial}{\partial r}\left(\frac{}{\partial r}\right)\cos\theta+\frac{\partial}{\partial r}\left(\frac{1}{r}\frac{\partial u_\theta}{\partial\theta}+\frac{\partial u_r}{\partial r}\right|\sin\theta\right]+F \qquad (5a)$$

$$\left\lfloor \frac{1}{r}\frac{(u_\theta)}{\partial \theta}+\frac{\rho u_r}{r}\right\rfloor (u_r \sin\theta + u_\theta \cos\theta)+\frac{1}{\varepsilon}\sqrt{u^2+u^2}\left(\frac{\partial(\rho u_r)}{\partial r}+\frac{1}{r}\frac{\partial(\rho u_\theta)}{\partial \theta}+\frac{\rho_{\ r}}{r}\right)=$$
$$=(-\varepsilon)\frac{\partial P}{\partial \theta}\frac{\cos\theta}{r}+\mu_e\left\lceil \frac{\partial}{\partial r}\left(\frac{}{\partial r}\right)\cos\theta + \frac{\partial}{\partial r}\left(\frac{1}{r}\frac{\partial u_\theta}{\partial \theta}+\frac{\partial u_r}{\partial r}\right)\sin\theta \right\rceil + F_\theta \tag{5b}$$

$$F_r = -\frac{\varepsilon\mu_e\rho}{K}(u_r\cos\theta - u_\theta\sin\theta)-\frac{\varepsilon F_\varepsilon}{\sqrt{K}}(u_r\cos\theta - u_\theta\sin\theta)\sqrt{u_r^2+u_\theta^2}+\varepsilon\rho g\beta(T-T_{\mathrm{ref}})\sin\theta \tag{5c}$$

$$F_\theta = -\frac{\varepsilon\mu_e\rho}{K}(u_r\sin\theta + u_\theta\cos\theta)-\frac{\varepsilon F_\varepsilon}{\sqrt{K}}(u_r\sin\theta + u_\theta\cos\theta)\sqrt{u_r^2+u_\theta^2}+\varepsilon\rho g\beta(T-T_{\mathrm{ref}})\cos\theta \tag{5d}$$

$$K = \frac{\varepsilon^3}{C(1-\varepsilon)^2} \tag{5e}$$

$$\lambda_t = (1-\varepsilon)\lambda_s + \varepsilon\lambda_l \tag{5f}$$

$$\frac{\partial(\rho H)}{\partial t}\quad \frac{1}{r^2}\frac{\partial}{\partial \theta}\left(l\frac{\partial}{\partial \theta}\right)+\frac{1}{r}\frac{\partial}{\partial r}\left(\lambda_l r\frac{\partial T}{\partial r}\right) \tag{6}$$

In order to characterize the non-linear relationship between wax evolution amount and temperature in the phase transition process of crude oil, combined with DSC curve test results, the enthalpy method is adopted to solve the liquid phase ratio change of crude oil. The calculation formulas were:

$$H(T) = c_{p\ j}T + \int_{T_N}^{T}(c_p(T)-c_{p,j})\mathrm{d}T \tag{7}$$

$$\varepsilon = 1 - \frac{H(T_j)-H(T)}{H(T_j)-H(T_N)} \tag{8}$$

Other layers of materials

The heat transfer equation of steel tube, insulation layer and protective layer were:

$$\rho_p c_{1,p}\frac{\partial T}{\partial t} = \frac{1}{r}\frac{\partial}{\partial r}\left(\lambda_1 r\frac{\partial T}{\partial t}\right)+\frac{\partial}{r^2\partial \theta}\left(\lambda_1\frac{\partial T}{\partial \theta}\right) \tag{9}$$

$$\rho_i c_i \frac{\partial T}{\partial t} = \frac{1}{r}\frac{\partial}{\partial r}\left(\lambda_2 r\frac{\partial T}{\partial t}\right)+\frac{\partial}{r^2\partial \theta}\left(\lambda_2\frac{\partial T}{\partial}\right) \tag{10}$$

$$\rho_e c_e \frac{\partial T}{\partial t} = \frac{1}{r}\frac{\partial}{\partial r}\left(\lambda_e r\frac{\partial T}{\partial t}\right)+\frac{\partial}{r^2\partial \theta}\left(\lambda_e\frac{\partial T}{\partial \theta}\right) \tag{11}$$

Boundary and initial conditions

$$-\lambda_1 \frac{\mathrm{d}T}{\mathrm{d}r}\Big|_{r=r4} = h(T-T_f)$$ (12)

$$T(r,\theta)\big|_{\tau=0} = T_{\text{in}}$$ (13)

Numerical prediction and verification

Shutdown experimental platform

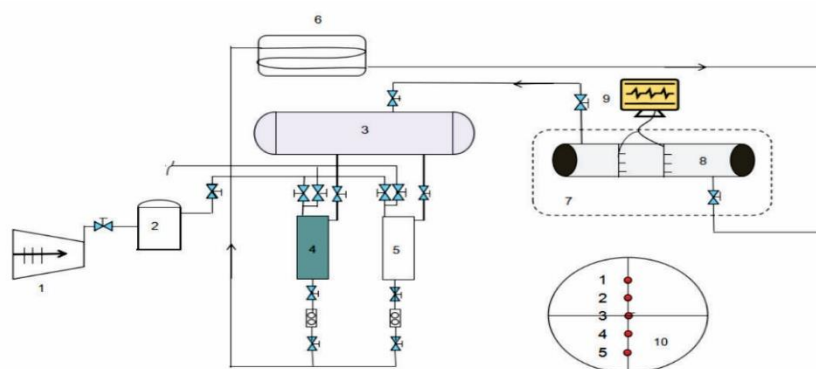The fig. 4 showed the flow diagram of the overhead pipeline shutdown laboratory.

Figure 4. Schematic diagram of hot oil pipeline test bench; *1 – compressor,*
2 – air bottle, 3 – oil-water separator, 4 – water bottle, 5 – oil bottle, 6 – heater,
7 – thermostat control cabinet, 8 – experimental section,
9 – data acquisition system, and 10 – thermocouple arrangement

The test stand consisted of two systems: the main circulation power system and the test system for closing the experimental pipe section. The main circulation power system included the oil-water separation system, the high pressure gas propulsion system and the heating system. The system included a thermostatic control system, a temperature test system and a data acquisition system. Two 4 mm diameter pipe supports were welded to the shutdown drive section. The temperature measurement points on each bracket were identical with five holes for thermocouples to pass through. The radial distance of each hole was 33 mm. To ensure that the thermocouples fixed to the brackets do not shift or fall off during the experiment, the brackets were insulated and sealed with resin glue. One end of the thermocouple was extended out of the tube by about 1 cm to reduce the influence of the holder on the temperature and flow fields. In the experiment, the arithmetic mean of the two corresponding temperature measurement points was used as the temperature at that point.

The main circulation system of the test bench was shown in fig. 5. In the main circulation system, the oil-water mixture was separated in the oil-water separator and then enters the oil and water tanks at its lower end, respectively. The high pressure gas heats the crude oil through the heater and pushes it into the experimental section. When the crude oil in the experimental section was filled with experimental oil, the circulating power system was shut down

506

Xu, Y., *et al.*: Study on Heat Transfer of Waxy Crude Oil Melting …
THERMAL SCIENCE: Year 2024, Vol. 28, No. 1B, pp. 1-14

Figure 5. The main circulation system of the test bench

for the shutdown experiment. After the crude oil solidifies in the pipeline, the heating and melting experiment was carried out by wrapping a thermostatic heating band around the outside of the experimental pipe section.

Numerical simulation
independence verification

The finite volume method was used to discretize the governing equations, and SIMPLE was used during the calculations. Figure 6 shows the verification of whether the grid numbers and time steps are independent.

It was easy to see from the three grid numbers that the grid number of the temperature curve was 6233, which was clearly different from the other curves, while the grid numbers of the crude oil temperature curve 8060 and 17136 almost overlapped. We further determined the grid number as 17136. when the calculation accuracy of the model reached the maximum, the grid number had no effect. Based on the determined grid number, the time step of the model was verified. Figure 6(b) showed the average temperature profiles of the pipe for time steps of 40 seconds, 20 seconds, and 10 seconds, respectively. It can be seen from the figure that the cooling curves with time steps of 10 seconds and 20 seconds basically overlapped, then we can determine that 10 seconds was a suitable time step when the number of grids was 17136.
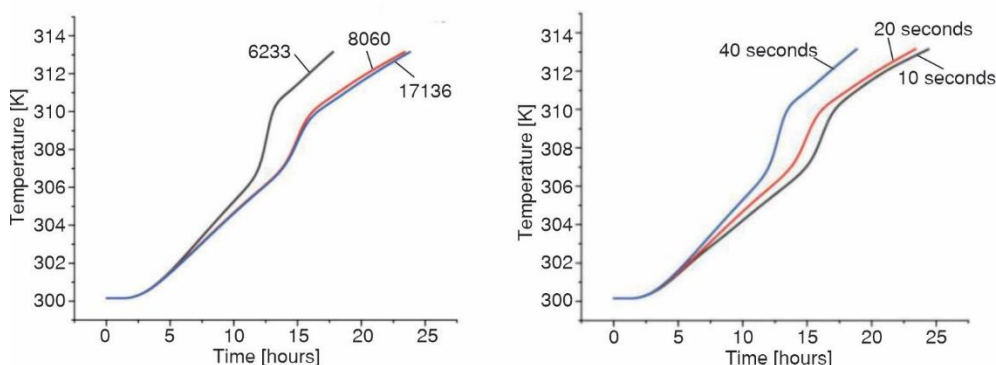

Figure 6. Average temperature curves of pipelines

Comparison of numerical and simulation results

The experiment pipe size was $\varnothing 219$ mm $\times$ 6 mm, and insulation material with a 20 mm thickness was applied on the outside. The physical parameters related to crude oil were

shown in the tab. 1, and relevant parameters such as pipes and insulation materials were shown in the tab. 2. The condensate oil temperature in the pipeline was 27 °C and uniformly distributed, the outer wall of the pipeline was heated at a constant temperature of 60 °C.

Table 1. Physical parameters of crude oil

Physical parameter	Formula
Equivalent instantaneous specific heat capacity	$c_p = \begin{cases} \left[0.1832 + 0.1006 \mathrm{e}^{\left[-0.5\left(\frac{T-300.87}{22.869} \right)^2 \right]} \right] 12004 & 257 < T < 322 \\ 2641 & T > 322\,\mathrm{K} \end{cases}$
Oil viscosity	$\mu = 821.5 \times 0.816^t,\ t > 43.6\ ^\circ\mathrm{C}$ $\mu = -0.11 + 801.5\mathrm{e}^{(-0.202t)},\ t \le 43.6\ ^\circ\mathrm{C}$
Oil density	$\rho_l = 882 - 0.5(t-20)$
Oil conductivity	Liquid oil: 0.15 W/mK, solid oil: 0.25 W/mK
Oil freezing point	32 °C
Oil coalescence point	38 °C

The comparison results of experiment and simulation were shown in the tab. 3.

It can be seen that in the whole process of heating and melting, the maximum relative error of the five positions was –5.23%, which indicated that the model and the solution method were correct.

Table 2. Physical parameters of other material

Material	Density	Conductivity	Specific heat capacity
	[kgm^{-3}]	[Wm^{-1}K^{-1}]	[Jkg^{-1}K^{-1}]
Steel pipe	7850	48	500
Insulation layer	60	0.04	700

Table 3. Comparison results of experiment and simulation

Time	Point 1			Point 2			Point 3			Point 4			Point 5		
	Cal.	Test	RE	Cal.	Test	RE	Cal.	Test	RE	Cal.	Test	RE	Cal.	Test	RE
Min.	°C	°C	%	°C	°C	%	°C	°C	%	°C	°C	%	°C	°C	%
30	27.0	27.0	–	27.5	27.0	1.8	27.0	27.0	–	27.0	27.0	–	27.4	28.1	–2.5
60	27.0	27.5	–1.9	29.2	28.6	2.1	27.0	27.0	–	27.0	27.0	–	29.2	30.3	–3.8
90	27.1	27.7	–2.2	40.4	39.1	3.2	27.0	27.0	–	27.1	27.3	–0.7	38.2	40.2	–5.23
120	27.7	28.4	–2.2	47.2	46.4	1.7	27.0	27.0	–	27.4	28.1	–2.5	40.5	41.5	–2.4
150	30.8	30.1	2.3	48.7	47.5	2.5	27.1	27.3	–0.7	28.3	29.2	–3.1	40.5	41.7	–3.0
180	44.8	42.8	4.46	49.9	49.1	1.6	27.3	28.1	–2.8	30.9	31.5	–1.9	40.2	41.7	–3.6
210	46.7	45.0	3.64	50.7	50.4	0.6	28.5	29.3	–2.7	38.8	39.4	–1.5	40.1	42.2	–2.6
240	48.0	47.1	2.1	51.5	51.0	1.0	43.9	44.6	–1.6	40.6	41.5	–2.2	40.1	42.4	–3.1
270	49.0	48.2	1.6	52.1	51.2	1.7	45.7	46.1	–0.9	42.7	43.9	–2.8	41.3	42.6	–3.1
300	49.9	49.5	0.8	52.7	52.2	1.0	47.2	48.1	–2.1	44.9	45.5	–1.3	43.2	43.9	–1.6

Analysis of the change of liquid phase in the melting process

Assuming that the crude oil in the pipeline had solidified after a period of time after the pipeline was shutdown, the temperature-adjustable heating belt was used to wrap around the steel pipe to melt the crude oil. When heated at 60 ℃ and at a constant temperature in the tropics, the changes in the melt liquid phase rate under different initial solidification states were shown in figs. 7 and 8.

As can be seen from fig. 7, the crude oil outside the pipe melts first during the heating and melting process outside the fully solidified pipe. The melted crude oil first lied in the voids
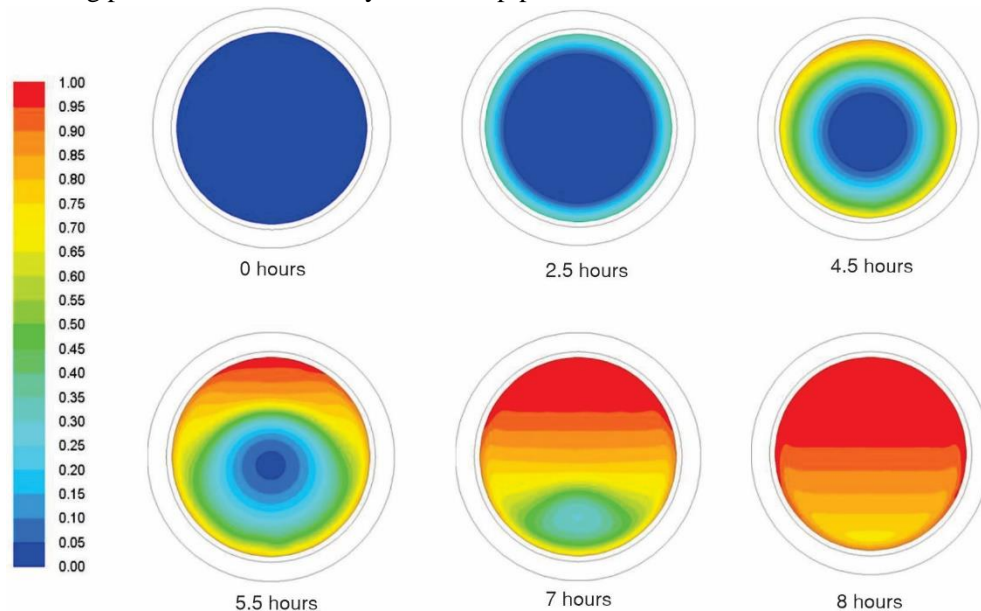

Figure 7. Cloud diagram of liquid rate change during the melting process of the fully solidified pipe

of the porous medium. Its movement was restricted by the solidified crude oil skeleton. Therefore, during the initial phase of heating, there was no significant relative motion throughout the pipeline. The oil melting in the pipeline was symmetrically distributed in an approximate circle (*e.g.*, cloud diagram for 2.5 hours). As the heating time increases, the grid structure disappeared when the temperature of the melted crude oil was higher than the temperature of the coalescence point (the temperature at which the porous medium was formed during the cooling of the crude oil). The melted crude oil had a clear natural convection effect, with the hot oil moving toward the upper wall of the pipe and the pure liquid crude oil concentrated in the upper part of the pipe. The low liquid-phase crude oil gradually migrates to the lower part of the pipeline due to its high relative density. During the downward migration, the condensate continuously absorbed heat and melted, resulting in a gradual increase in the overall liquid phase ratio of crude oil in the pipeline and an increasing proportion of pure liquid phase crude oil. When heated for 8 hours, the pure liquid crude oil had basically occupied the upper part of the pipeline. With the extension of heating time, the interface shape of different liquid phase rates changed in different ways. The interface of the low liquid phase mainly changed from circular to elliptical, while the interface of the high liquid phase gradually changed from curved to straight.

From fig. 8, it can be seen that for the pipeline containing some liquid crude oil, when heating was performed outside the pipeline, the center of the pipeline was a relatively high liquid phase rate region in the initial stage of heating. With the extension of heating time, the liquid phase near the inner wall of the pipe gradually increased, and the high liquid phase region gradually concentrated on the upper wall of the pipe and started to spread downward. During the whole melting process, due to the natural convection between the high liquid crude oil zone inside the pipeline and the liquid crude oil near the inner wall of the pipeline, the high temperature crude oil inside and outside the condensate layer was concentrated near the upper wall of the pipeline, resulting in the first disappearance of the condensate layer near the upper wall of the pipeline, thus forming a "gap" and a "crescent-shaped" low liquid phase separation interface in the lower part of the pipeline. With the extension of heating time, the "crescent-shaped" area gradually disappeared and formed an elliptical area, which kept moving toward the lower wall of the pipeline and formed an approximately horizontal liquid rate interface with the upper wall of the pipeline.
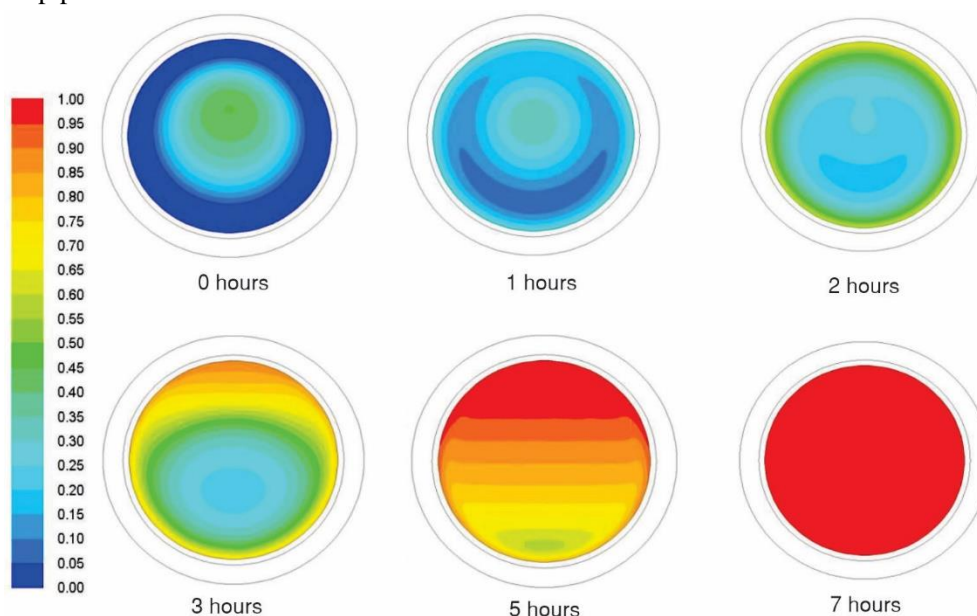

Figure 8. Cloud diagram of liquid rate change in the melting process for the initial liquid rate of 0.15

When the temperature was fixed to 60 ℃ in the heating belt, for three different initial liquid phase rates, 0 (full condensate pipeline), 0.15 and 0.5, respectively, the liquid phase rate changes during heating and melting were shown in the fig. 9.

It can be seen from fig. 9 that the trend of the overall liquid phase rate during melting was basically the same at different initial solidification states during constant temperature heating. The difference lied in the different trends of curve changes in the initial stage of heating. The specific analysis was as follows:

– For the pipeline with initial full condensation (*i.e.*, the initial liquid phase rate is 0), when all the crude oil in the pipeline was solidified, the crude oil near the pipeline wall was far below the freezing point. Therefore, in the initial stage of heating, this part of the crude oil needed to absorb a large amount of heat to reach the melting point.

510

Xu, Y., *et al.*: Study on Heat Transfer of Waxy Crude Oil Melting …
THERMAL SCIENCE: Year 2024, Vol. 28, No. 1B, pp. 1-14

– For the pipeline where most of the crude oil had solidified before heating (initial liquid rate of 0.15), the center of the pipeline was liquid crude oil. In the initial stage of heating, the solid crude oil absorbed additional heat from the tropics in the pipe, while the high temperature central liquid crude oil was losing heat to the condensate layer due to the presence of radial temperature difference. At this time, the condensate in the middle had not yet reached the melting temperature, and the liquid crude oil in the center of the pipeline cooled rapidly to the freezing point due to the small amount and rapid heat dissipation, so there was a short period of decline in the liquid phase rate in the initial stage.

– For the pipeline with less initial condensate (liquid phase rate of 0.5), the temperature of the initial condensate layer was relatively high compared with the pipeline with a lower initial liquid phase rate, and the heat storage of crude oil in the liquid region was relatively large, resulting in a less pronounced decreasing trend of the liquid phase rate in the initial stage.

For the initial liquid phase ratio of 0.15 pipeline, the temperature rise curves of crude oil at typical positions in the pipeline were shown in the fig. 10.
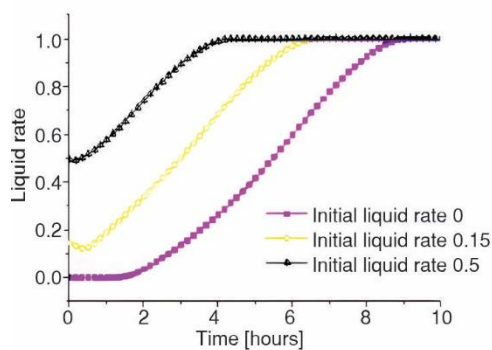

Figure 9. Changes of liquid rate in melting process under different solidification conditions
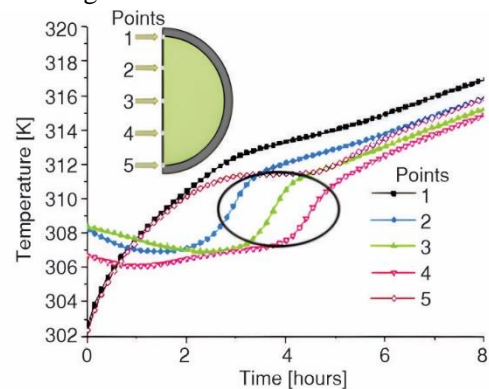
Figure 10. Temperature rise curves at typical locations

In fig. 10, the crude oil close to the tube wall (Points 1 and 5) was near the heat source and was heated continuously, so the heating temperature profile rose rapidly and the temperature rise rates at both points were equal. Later, the temperature rise rate at Point 1 was higher than that at Point 5 as the melted hot oil near the pipe wall moved toward the upper part of the pipe wall. The melted hot oil moved rapidly to the upper part of the pipe due to its high temperature and low density, resulting in an asymmetric temperature distribution of crude oil at symmetrical locations above and below the *Y*-axis of the pipe. The temperature at the upper part is higher than the lower part, so the temperature at Point 2 was always higher than the temperature at Point 4. In addition, the crude oil located inside the pipe (Points 2, 3, and 4) dissipated heat radially to the vicinity of the pipe wall because its initial temperature was higher than that of the low temperature condensate near the pipe wall. At this time, the heat in the heating zone was mainly concentrated in the crude oil near the molten pipe wall and was not fully transferred to the inside of the pipe, so the temperature of the crude oil at these locations decreases during the initial heating phase. As the heating time increases, this part of the crude oil started to absorb latent heat and the temperature rose slowly. When the temperature of the crude oil exceeded the freezing point (305 K), the temperature rise rate increased sharply, which was due to the transition of the crude oil from the solidified state to the porous medium state. After the formation of the fuzzy zone in the porous medium, the external flow of the melted

crude oil can accelerate the melting of the solid skeleton, and the rapid mixing of the melted cold oil and hot oil also leaded to the sudden increase of the crude oil temperature here.

Conclusion

In this paper, based on the microscopic aggregation behavior of wax crystals in the phase change process, a novel mathematical model of thermal melting and heat transfer of crude oil in long-distance pipelines was established, which can accurately describe the physical phenomena involved in the phase change process of crude oil, such as mobile phase interface, liquid-solid coupling, latent heat release, and natural convection. An experimental platform was built for the shutdown pipeline and a heating and melting experiment was conducted for condensate. After comparing the experimental results with the simulation results, the correctness of the model and its solution method were verified. Based on the overall solidified pipeline and the partially solidified pipeline, the variation law of the liquid phase ratio during the melting of crude oil in the pipeline was analyzed, and the melting process and heat transfer characteristics were determined. The results of this study can be used to guide the heating and melting engineering of crude oil condensate pipeline.

Acknowledgment

Nomenclature

c_i – specific heat capacity of insulating layer, $[\mathrm{Jkg^{-1}K^{-1}}]$

$c_{1,p}$ – specific heat capacity of pipe, $[\mathrm{Jkg^{-1}K^{-1}}]$

c_p – transient equivalent specific heat capacity of crude oil, $[\mathrm{Jkg^{-1}K^{-1}}]$

F_s – shape coefficient

F_ε – shape factor

g – gravitational acceleration, $[\mathrm{ms^{-2}}]$

H – enthalpy value, $[\mathrm{Jkg^{-1}}]$

K – permeability

P – apparent stress, [Pa]

r_1 – pipe radius, [m]

r_2 – outer radius of pipe/inner radius of insulation material, [m]

r_3 – outside radius of insulation, [m]

T – oil temperature, [K]

T_{ref} – reference temperature, [K]

t – shutdown time, [hours]

Greek symbols

β – expansion coefficient, [1/K]

ε – liquid fraction

λ_1 – pipe thermal conductivity, $[\mathrm{Wm^{-1}K^{-1}}]$

λ_2 – thermal conductivity of insulation, $[\mathrm{Wm^{-1}K^{-1}}]$

λ_l – thermal conductivity of liquid crude oil, $[\mathrm{Wm^{-1}K^{-1}}]$

λ_s – thermal conductivity of liquid crude oil, $[\mathrm{Wm^{-1}K^{-1}}]$

λt – effective thermal conductivity, $[\mathrm{Wm^{-1}K^{-1}}]$

μ – kinematic viscosity, $[\mathrm{kgm^{-1}s^{-1}}],[\mathrm{Pa \cdot s}]$

ρ – oil density, $[\mathrm{kgm^{-3}}]$

ρ_i – insulating layer density, $[\mathrm{kgm^{-3}}]$

ρ_p – pipe density, $[\mathrm{kgm^{-3}}]$

φ – solid fraction

References

[1] Hong, Q. J, *et al*., A Pore-Scale Visualized Study of Melting Heat Transfer of a Paraffin Wax Saturated in a Copper Foam: Effects of the Pore Size, *Int. J. Heat Mass Transfer, 112* (2017), Sept., pp. 39-44

[2] Korawan, A. D., *et al*., 3D Numerical and Experimental Study on Paraffin Wax Melting in Thermal Storage for the Nozzle-and-Shell Tube-and-Shell, and Reducer-and-Shell Models. *Model Simul. Eng., 2017* (2017), ID9590214

[3] Wei, H., *et al.*, Optimal Thermal Management of Server Cooling System Based Cooling Tower Under Different Ambient Temperatures, *Applied Thermal Engineering, 207* (2022), May, pp. 118-176

512

Xu, Y., *et al.*: Study on Heat Transfer of Waxy Crude Oil Melting …
THERMAL SCIENCE: Year 2024, Vol. 28, No. 1B, pp. 499-512

[4] Seddegh, S., *et al.*, Numerical Investigation of Heat Transfer Mechanism in a Vertical Shell and Tube Latent Heat Energy Storage System, *Applied Thermal Engineering*, *87* (2015), Aug., pp. 698-706

[5] Mao, Q., Zhang, Y., Thermal Energy Storage Performance of a Novel Three-PCM Cascade Tank in a High-Temperature Packed Bed System. *Renewable Energy*, *152* (2020), June, pp. 110-119

[6] Xu, Y., *et al*., Effects of Crude Oil's Variable Physical Properties on Temperature Distribution in a Shutdown Pipeline, *Advances in Mechanical Engineering*, *9* (2017), 4, pp. 1-9

[7] Xu, Y., *et al*., Heat Transfer Analysis of Waxy Crude Oil Under a New Wide Phase Change Partition Model, *Numerical Heat Transfer, Part A: Applications*, *76* (2019), 12, pp. 991-1005

[8] Yu, G. J., *et al*., A New General Model for Phase-Change Heat Transfer of Waxy Crude Oil During the Ambient Induced Cooling Process, *Numerical Heat Transfer, Part A, 71* (2017), 5, pp. 511-527

[9] Mao, Q., *et al*., Study on the Influence of Tank Structure and Fin Configuration on Heat Transfer Performance of Phase Change Thermal Storage System, *Energy, 235* (2021), 121382

[10] Drissi, S., *et al*., Thermal Analysis by DSC of Phase Change Materials, Study of the Damage Effect, *Journal of Building Engineering*, *1* (2015), Mar., pp. 13-19

[11] Sun, X. Q., *et al*., Experimental Observations on the Heat Transfer Enhancement Caused by Natural Convection During Melting of Solid-Liquid Phase Change Materials (PCMs), *Applied Energy*, *162* (2016), Jan., pp.1453-1461

[12] Kousksou, T., *et al*., An Implicit Enthalpy Formulation for Macroscopic Eutectic and Progressive Melting: DSC (Differential Scanning Calorimetry) Applications, *Energy*, *66* (2014), Mar., pp. 919-926

[13] Chen, W.-H., Jiang, L.-L., Numerical Simulation of New Phase-change Finned Tube Heat Accumulators (in Chinese). *Chemical Machinery*, *38* (2011), 6, pp. 730-733

[14] Jin, R.-F., *et al*., Numerical Simulation of Discharging Process for a Shell-tube Phase Change Thermal Storage (in Chinese), *Building Energy & Environment*, *28* (2009), 1, pp. 14-17

[15] Ma, C., *et al*., Electrical Treatment of Waxy Crude Oil to Improve Its Cold Flowability, *Industrial & Engineering Chemistry Research*, *56* (2017), 38, pp. 10920-10924

[16] Lize, M. S. L., Oliveira, *et al*., Wax Behavior in Crude Oils by Pour Point Analyses, *Braz. Chem,Soc, 29* (2018), 10, pp. 2158-2168

[17] Paska, J., *et al*., Hybrid Power Systems – An Effective Way of Utilising Primary Energy Sources, *Renewable Energy*, *34* (2009), 11, pp. 2414-2421

[18] Mao, Q., Recent Developments in Geometrical Configurations of Thermal Energy Storage for Concentrating Solar Power Plant, *Renewable & Sustainable Energy Reviews*, *59* (2016), June., pp. 320-327